A Discrete-Time Approach to Analyze Hard Handoff Performance in Cellular Networks

Alexe E. Leu, *Member, IEEE,* and Brian L. Mark, *Member, IEEE*

***Abstract*—The handoff algorithm employed in a cellular network has a significant impact on overall network performance, but evaluation of handoff performance has for the most part been done using only crude approximations or brute-force computer simulation. We introduce a new discrete-time approach to analyze the performance of handoff algorithms based on pilot signal strength measurements. We derive exact analytical expressions and develop a recursive numerical procedure to evaluate handoff performance metrics for a mobile station moving along a straight-line trajectory in a cellular network employing hard handoff. The numerical procedure provides a computational solution to a level-crossing problem in discrete time. Our discrete-time approach provides valuable analytical insight into the performance impact of handoff algorithms. Moreover, our numerical procedure for discrete-time handoff analysis provides an accurate and efficient tool for the design and dimensioning of high-performance handoff algorithms. The accuracy of the numerical procedure is validated by simulation.**

***Index Terms*—Cellular systems, discrete-time systems, handoff algorithms, level-crossing problems.**

I. Introduction

IN CELLULAR networks, each mobile station (MS) maintains connectivity via an active set of base stations (BS). A handoff algorithm determines the dynamics of the active set as the MS moves through the network. In hard handoff, the MS is "handed off" from one BS to another BS as it leaves the cell coverage area of the first and enters that of the second. In this case, the active set of an MS consists of at most one BS at any given time. Hard handoff algorithms are used in 2G and 3G wireless networking standards such as GSM, GPRS, and UMTS (FMA1 mode) [1].

The handoff behavior of mobile units in a cellular network is critical to the overall performance in terms of quality of service, resource utilization, and signaling load. Ideally, the network should maintain a seamless quality of service for an active mobile user engaged in a call as it traverses cell boundaries. Even when the mobile station is in the idle state, handoff decisions impact the network in terms of resource utilization and signaling load as well as the quality of service experienced by the MS when it transits to the active state. Thus, the proper design and dimensioning of the handoff algorithm is crucial to the deployment of a cellular network. The present paper is motivated by the need for an analytical framework to model handoff behavior accurately and to dimension parameter values without resorting to time-consuming computer simulation.

We develop a new discrete-time approach to analyze the handoff performance of an MS moving along a trajectory in a cellular network. The handoff decisions are based on pilot signal strength measurements from the candidate BSs. Handoff behavior is characterized in terms of events associated with a discrete-time random process (i.e., a random sequence) determined by the received pilot signal strengths from the candidate BSs. Our discrete-time framework allows us to derive exact expressions for the cell assignment and handoff probabilities at each sampling epoch along a trajectory traversed by the MS. Based on the discrete-time approach, we develop an efficient numerical procedure to compute handoff performance measures such as the handoff and assignment probabilities of the MS. Such a procedure can be used to design and dimension the parameters for handoff in a cellular network. Our analytical approach also provides new insights into the behavior and performance of handoff algorithms. In particular, our analysis reveals the effect of the averaging filter for the received pilot signal strengths on the handoff decisions.

Early work on handoff performance evaluation has largely been based on computer simulation studies [2]–[5]. In industrial practice, computer simulation remains the primary means for choosing key parameters to optimize the performance of modern-day wireless networks. Detailed computer simulations of wireless cellular networks require considerable computation time, making them cumbersome to use for the purposes of network design and dimensioning. More importantly, the simulation approach generally does not lead to deeper analytical insight into handoff performance.

The present paper was inspired by earlier work of Holtzman and his coworkers [6], [7], who were among the first to attempt an analytical study of handoff performance along a mobile trajectory. Vijayan and Holtzman [6] characterized handoff behavior in terms of the level crossings of the difference in the received pilot signal strengths of two candidate BSs. In the asymptotic regime of high-level crossings, the level-crossing events form a Poisson process. Two limitations of the Poisson level-crossing model are that it is accurate only for relatively high-level crossings and the sampling interval must be sufficiently small for the continuous-time model to be accurate. Subsequently, Zhang and Holtzman [7] proposed a discrete-time approach to analyze handoff based on the Gaussian properties of the sampled and processed received signal strengths. The formulas obtained in [7] rely on simplifying

Manuscript received November 9, 2002; revised May 9, 2003; accepted June 9, 2003. The editor coordinating the review of this paper and approving it for publication is Q. Zhang. This work was supported in part by the National Science Foundation under Grant ACI-0133390 and by the TRW Foundation.

A.E. Leu is with the Shared Spectrum Company, Vienna, VA, 22812 USA (e-mail: aleu@sharedspectrum.com).

B. L. Mark is with the Department of Electrical and Computer Engineering, George Mason University, Fairfax, VA 22030 USA (e-mail: bmark@gmu.edu).

Digital Object Identifier 10.1109/TWC.2004.833480

approximations that can lead to inaccurate results, as we have observed in our numerical studies. The discrete-time handoff analysis developed in the present paper differs from those of [6] and [7] in that it does not involve any approximations, given the basic system model. In essence, our approach provides a solution to the level-crossing problem in the discrete-time domain.

While handoff algorithms have been studied extensively in recent years (cf., [8]–[10]), to our knowledge ours is the first exact analytical framework for computing the handoff performance measures considered in [6] and [7], i.e., assignment and handoff probabilities along a mobile trajectory. In [11], the mean number of handoffs for an MS moving between two BSs is evaluated via simulation and a simple closed-form approximation is developed by curve-fitting to the simulation results. In [12], a similar approach is used to obtain a simple closed-form expression for the mean handoff delay. The expression is exact when the hysteresis margin is zero but is only approximate when a nonzero hysteresis margin is included. Indeed, the authors of [12] state that finding an exact analytic expression for the cell assignment probability "does not seem tractable." In [13], the rate of switching between BSs for an MS is analyzed, but the authors do not address the "difficult problem of a handoff algorithm utilizing hysteresis to reduce handoff rate." Thus, our discrete-time approach provides a solution to an important open problem in handoff design.

Other recent works related to handoff analysis have focused on traffic modeling and call blocking probability during handoff (cf., [14] and [15]) in the spirit of earlier traffic-based models used to study the performance of cellular networks (cf., [16] and [17]). Typically, the traffic models used in conjunction with handoff studies assume Poisson call arrivals. In contrast, our work makes no assumptions on the traffic arrival processes and focuses exclusively on modeling the handoff behavior of an MS moving along a particular trajectory in the network based on received signal strength measurements.

Section II describes the basic signal propagation model for a general class of handoff algorithms, first in the more familiar continuous-time setting and then in discrete-time, providing the basis for our subsequent analysis. Section III introduces a new discrete-time formulation of the handoff problem and develops analytical expressions for the handoff performance measures in discrete time. Section IV develops an efficient recursive procedure for computing the handoff performance measures. Section V presents numerical evaluations of handoff performance obtained using the discrete-time approach. Finally, the paper is concluded in Section VI.

II. Pilot Signal Strength Model

This section describes the signal propagation model for the pilot signal strength used by handoff algorithms. The propagation model provides the basis for analyzing the handoff performance of an MS travelling along a straight-line trajectory at constant speed in a cellular network. A discrete-time version of this model is used in our subsequent analysis of handoff performance.

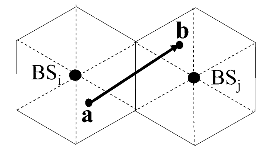

Fig. 1. Straight-line trajectory between two BSs in a cellular network.

A. Continuous-Time Model

The cellular network consists of a set of BSs. The ith station BS_i, located by a position vector $\mathbf{b}_i$, lies at the center of its associated cell i. The coverage area of cell i is determined by the pilot signal strength from BS_i. Assume that the MS is initially located at position $\mathbf{a}$ at time zero and connected to BS_i. The MS reaches position $\mathbf{b}$ at time T, moving at a constant speed of v along the line segment between $\mathbf{a}$ and $\mathbf{b}$. As the MS moves along this trajectory, the candidate BS for handoff is BS_j (see Fig. 1). The MS makes handoff decisions based on measurements of the pilot signal strengths received from the two BSs BS_i and BS_j. The position $\mathbf{r}(t)$ of the MS at time t is given as follows:

$$\mathbf{r}(t) = \mathbf{a} + vt\mathbf{e}, \quad 0 \le t \le T$$

where $\mathbf{e}$ is the unit vector in the direction of the vector $\mathbf{b} - \mathbf{a}$.

The pilot signal strength (in decibels) received from a BS as a function of distance in typical urban mobile environments has been modeled empirically as the sum of three components (cf., [18]): path loss, shadow fading, and fast fading. The path loss is a deterministic function of the distance d from the BS, while the shadow and fast-fading components are modeled as random processes in the distance parameter d. This model has been used in a number of studies of handoff performance in cellular networks (cf., [6]). Under the assumption of constant MS speed along the straight-line trajectory, the pilot signal strength can be expressed equivalently as a function of a continuous-time parameter t. The pilot signal strength (in decibels), received at the MS from BS_i at time t, is represented as follows:

$$Y_i(t) = m_i(t) + W_i(t) + Z_i(t), \quad t \ge 0 \tag{1}$$

where

$$m_i(t) = \kappa_1 - \kappa_2 \log(\|\mathbf{r}(t) - \mathbf{b}_i(t)\|) \tag{2}$$

and $\{W_i(t)\}$, $i \in \mathcal{C}$ are independent[1] zero-mean stationary Gaussian processes. The values of the constants κ_1 and κ_2 depend on the mobile environment, with $\kappa_1 = 0$ dB and $\kappa_2 = 30$ dB being typical values in an urban setting. The term $m_i(t)$ accounts for path loss, while $W_i(t)$ models the effect of lognormal (shadow) fading and $Z_i(t)$ models fast fading. The autocorrelation function of $W_i(t)$ has been experimentally observed to have the following form (cf., [18]):

$$R_{W_i}(\tau) = \sigma_{W_i}^2 \exp\left(-\frac{v|\tau|}{d_0}\right) \tag{3}$$

[1]If necessary, cross correlation between received signal strengths can easily be incorporated into the model.

where σ_{W_i} is the standard deviation of the shadowing signal strength and the constant d_0 is called the decay factor.

To eliminate the effect of fast fading, the MS applies an exponential averaging window to the measured signal strength $Y_i(t)$. The impulse response of the averaging window is given by

$$f_{\rm av}(t) = \frac{1}{d_{\rm av}} \exp\left(-\frac{vt}{d_{\rm av}}\right), \quad t \geq 0 \tag{4}$$

where $d_{\rm av}$ determines the effective size of the averaging window. The processed pilot signal strength from BS_i is then given by $X_i(t) = f_{\rm av}(t) \star Y_i(t)$, where $\star$ denotes convolution.

B. Discrete-Time Model

Our analysis of handoff performance is based on a discrete-time model for the signal strength measurements. In the discrete-time model, the mobile unit samples the pilot signal strengths at time instants $t_k = kt_s$, where t_s is the sampling interval. The discrete-time parameter k varies between zero and $K = \lfloor T/t_s \rfloor$, the total number of sampling intervals along the MS trajectory from time zero and to time T. The distance between successive sampling positions of the mobile is denoted by $d_s = vt_s$. The discrete-time model captures the handoff behavior of an MS more accurately than its continuous-time counterpart since all signal strength measurements are sampled in an actual system.

In discrete time, the basic signals of the system model are simply sampled versions of their continuous-time counterparts

$$Y_i[k] = Y_i(t_k), \quad m_i[k] = m_i(t_k), \quad W_i[k] = W_i(t_k). \tag{5}$$

The processes $\{W_i[k]\}$, $i \in \mathcal{C}$, are independent zero-mean stationary Gaussian processes characterized by an autocorrelation function given by

$$R_{W_i}(l) = \sigma_{W_i}^2 \exp\left(-\frac{|l|d_s}{d_0}\right). \tag{6}$$

The shadow fading process $\{W_i[k]\}$ can be represented as a first-order autoregressive (AR) process by the following:

$$W_i[k] = aW_i[k-1] + V_i[k], \quad k \geq 0 \tag{7}$$

where $\{V_i[k]\}$ is a zero-mean stationary white Gaussian noise process with variance $\sigma_{V_i}^2$. The parameters $(a, \sigma_{V_i}^2)$ of the AR model determine an autocorrelation function for $\{W_i[k]\}$ of the form

$$R_{W_i}(l) = \sigma_{V_i}^2 \frac{a^{|l|}}{1-a^2}. \tag{8}$$

By comparing (6) and (8), the AR parameters for the shadow fading process are determined as

$$a = \exp\left(-\frac{d_s}{d_o}\right), \quad \sigma_{V_i}^2 = (1-a^2)\sigma_{W_i}^2.$$

The discrete-time equivalent of the exponential smoothing window is given by

$$f_{\rm av}[k] = \frac{d_s}{d_{\rm av}} \exp\left(-\frac{kd_s}{d_{\rm av}}\right) = \frac{b^k}{d_{\rm av}}, \quad k \geq 0 \tag{9}$$

where $b = \exp(-d_s/d_{\rm av})$. The processed pilot signal strength $X_i[k]$ from BS_i is then obtained by convolving $f_{\rm av}[k]$ with $Y_i[k]$ in the discrete-time domain. The evolution of the process $\{X_i[k]\}$ is governed by the following second-order difference equation (see Appendix I):

$$\begin{aligned} X_i[k] =& (a+b)X_i[k-1] - abX_i[k-2] \\ &+ \frac{d_s(m_i[k] - am_i[k-1] + V_i[k])}{d_{\rm av}} \\ k \geq& 2. \end{aligned} \tag{10}$$

From (10), we see that $\{X_i[k]\}$ is a second-order AR process, a fact that we shall exploit in Section III. Various statistical properties of the process $\{X_i[k]\}$ that will be used in the sequel are derived in Appendixes I and II.

III. Discrete-Time Handoff Analysis

A. Assignment Regions

The MS makes a handoff decision based on the processed pilot signal strengths from the two candidate BSs. In other words, a handoff decision made at time k is based on the vector $\mathbf{X}[k] = (X_j[k], X_i[k]) \in \mathcal{R}^2$, where $\mathcal{R}$ denotes the real line. A large class of so-called hysteresis-based handoff algorithms may be characterized in terms of a partition of $\mathcal{R}^2$ into three regions: $\mathbf{I}$ is the assignment region for BS_i; $\mathbf{J}$ is the assignment region for BS_j; and $\mathbf{H}$ is the hysteresis region, where the MS may be assigned either to BS_i or BS_j.

A handoff decision at time $k > 0$ is made as follows.

1) If $\mathbf{X}[k] \in \mathbf{I}$, then a handoff occurs to BS_i unless the MS is already assigned to BS_i.
2) If $\mathbf{X}[k] \in \mathbf{J}$, then a handoff occurs to BS_j unless the MS is already assigned to BS_j.
3) If $\mathbf{X}[k] \in \mathbf{H}$, then no handoff occurs.

At time $k = 0$ the MS becomes active and is assigned to BS_i, if $X_i[0] \geq X_j[0]$, and otherwise to BS_j. In this case, the hysteresis level is effectively zero and there are only two assignment regions: $\mathbf{I}_0 = \{(x_j, x_i) : x_i \geq x_j\}$ is the assignment region for BS_i at time zero and $\mathbf{J}_0 = \{(x_j, x_i) : x_i < x_j\}$ is the assignment region for BS_j at time zero.

With the above formulation of hysteresis-based handoff, we may consider some important special cases. A practical class of handoff algorithms operates on the basis of the *relative* processed signal strength from BS_i and BS_j (cf., [6]). We define hysteresis levels h_i and h_j associated with BS_i and BS_j, respectively. A handoff of the mobile user from BS_i to BS_j occurs when the relative processed signal strength

$$X_\Delta[k] \triangleq X_i[k] - X_j[k]$$

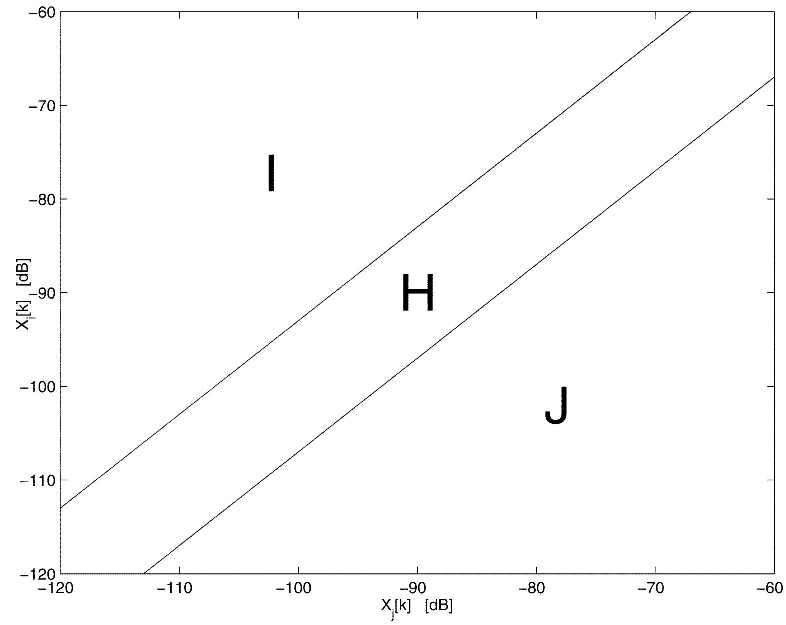

Fig. 2. Assignment regions based on relative signal strength.

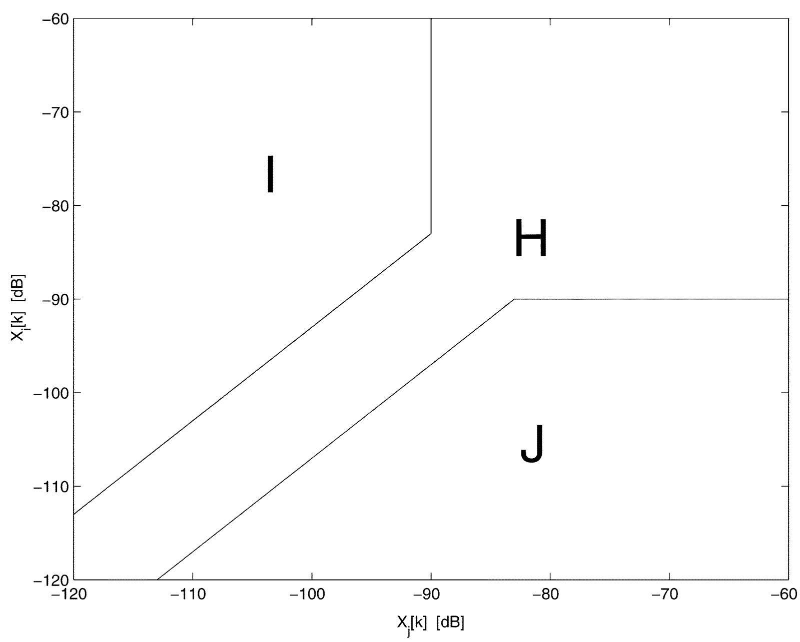

Fig. 3. Assignment regions based on relative strengths with absolute thresholds.

falls below the value $-h_j$. Conversely, a handoff from BS_j to BS_i occurs when $X_\Delta[k]$ exceeds the value h_i. For handoff algorithms based on relative signal strength, the assignment regions are given as follows: $\mathbf{I} = \{(x_j, x_i) : x_i \geq x_j + h_i\}$, $\mathbf{J} = \{(x_j, x_i) : x_i \leq x_j - h_j\}$, and $\mathbf{H} = \mathcal{R}^2 - (\mathbf{I} \cup \mathbf{J})$, where "$-$" denotes the set difference operator. These regions are illustrated in Fig. 2.

Some handoff algorithms combine relative signal strength with an absolute threshold on the required pilot signal strength (cf., [7]). In such algorithms, a handoff from BS_i to BS_j occurs at time k if and only if $X_\Delta[k] \leq -h_j$ and $X_i[k] < T_i$, where T_i is the absolute threshold on $X_i[k]$. Conversely, a handoff from BS_j to BS_i occurs at time t if and only if $X_\Delta[k] \geq h_i$ and $X_j[k] < T_j$. The two-dimensional (2-D) assignment regions for this handoff algorithm become: $\mathbf{I} = \{(x_j, x_i) : x_i \geq x_j + h_i, x_j < T_j\}$, $\mathbf{J} = \{(x_j, x_i) : x_i \leq x_j - h_j, x_i < T_i\}$, and $\mathbf{H} = \mathcal{R}^2 - (\mathbf{I} \cup \mathbf{J})$. These regions are illustrated in Fig. 3. Different specifications of the assignment regions lead to different handoff algorithms. A nonlinear assignment region is illustrated in Fig. 4. A nonlinear assignment region arises, for example, in the locally optimal handoff algorithm described in [19].

B. Handoff as a Level-Crossing Problem

The handoff behavior of an MS traveling along a given trajectory can be viewed as a 2-D level-crossing problem (cf., [20]). Handoff events may occur when the process $\mathbf{X}[k]$ enters the assignment regions $\mathbf{I}$ and $\mathbf{J}$. The level-crossing analogy can be more readily visualized in the case of handoff based on relative

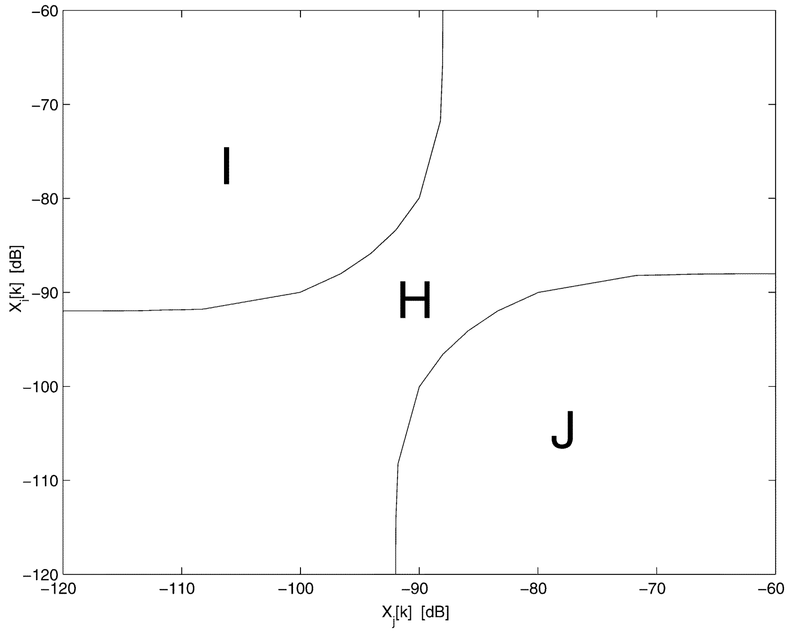

Fig. 4. Nonlinear assignment regions.

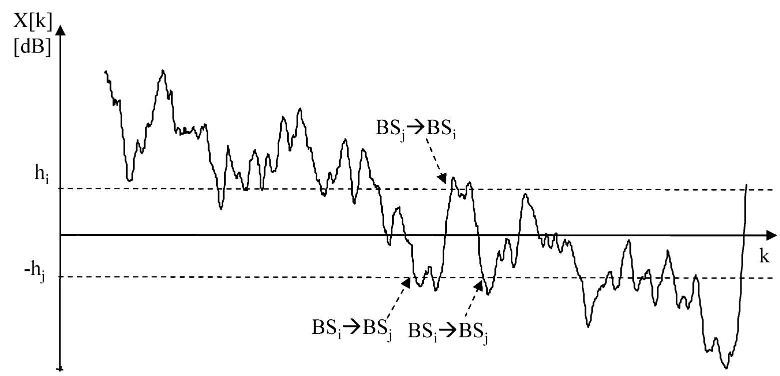

Fig. 5. Handoff as a level-crossing problem.

signal strength. In this case, the handoff decision is based on the one-dimensional (1-D) relative signal strength $X_{\Delta}[k]$. Handoff events correspond to level crossings of the process $X_{\Delta}[k]$ with respect to the hysteresis levels h_i and $-h_j$. Thus, handoffs from BS_i to BS_j correspond to downcrossings of $-h_j$, while handoffs from BS_j to BS_i correspond to upcrossings of h_i, as can be seen in Fig. 5.

The handoff analysis of Vijayan and Holtzman [6] is based on the level-crossing analogy in the 1-D case and in the continuous-time domain. In the asymptotic regime where $h_i, h_j \to \infty$, the point process formed by the set of upcrossings of h_i and that formed by the set of downcrossings of $-h_j$ approach independent Poisson processes [20]. Based on this result, Vijayan and Holtzman obtain expressions for handoff performance metrics such as handoff probability and cell assignment probability. However, the Poisson process model is generally not accurate for smaller values of the hysteresis levels.

In practice, as the MS moves along a given trajectory, it samples and processes the signal strengths from the candidate BSs at discrete time instants. Level crossings between sampling instants do not necessarily lead to actual handoff events. The analysis in [6] relies on the assumption that the sampling interval is sufficiently small such that at most one level-crossing event can occur between sampling instants. Thus, the analysis based on the continuous-time model cannot capture the effect of varying the sampling interval on handoff behavior. The approach to handoff analysis introduced in this paper provides, in effect, a solution to the level-crossing problem in discrete time, which captures the behavior of practical handoff algorithms.

C. Assignment Probability

We represent the sampled and processed signal strength measurements from BS_i and BS_j by the vector process $\mathbf{X}[k] = (X_j[k], X_i[k])$. Let $\mathbf{X}[k \backslash r]$ denote the sequence consisting of the r most recent values of $\{\mathbf{X}[k]\}$ up to and including time k, where $1 \le r \le k+1$

$$\mathbf{X}[k \backslash r] = (\mathbf{X}[k-r+1], \mathbf{X}[k-r+2], \ldots \mathbf{X}[k]). \quad (11)$$

Equivalently, $\mathbf{X}[k \backslash r]$ may be viewed as a string of length r on the alphabet

$$\mathcal{A} = \{\mathbf{I}_0, \mathbf{I}, \mathbf{J}_0, \mathbf{J}, \mathbf{H}\}.$$

We shall use the notation $\mathbf{H}^r$ to denote a string consisting of the symbol $\mathbf{H}$ repeated r times. When $k=0$, $X[k]$ falls in either region $\mathbf{I}_0$ or region $\mathbf{J}_0$. At any time $k \geq 1$, the vector $\mathbf{X}[k]$ falls in exactly one of the three assignment regions $\mathbf{I}$, $\mathbf{J}$, or $\mathbf{H}$.

Cell assignment of an MS along a given trajectory can be characterized as follows. For $k \geq 1$, if the MS is assigned to BS_i at time $k-1$, a handoff to cell j occurs at time k if and only if $\mathbf{X}[k] \in \mathbf{J}$. Conversely, if the MS is assigned to BS_j at time $k-1$, a handoff to cell i occurs at time k if and only if $\mathbf{X}[k] \in \mathbf{I}$. We can also characterize cell assignment as follows.

Proposition 1: At time $k \geq 1$, the MS is assigned to BS_i if and only if $\mathbf{X}[k \backslash k+1] \in \mathbf{I}_0\mathbf{H}^k$ or $\mathbf{X}[k \backslash r] \in \mathbf{I}\mathbf{H}^{r-1}$ for some r, $1 \leq r \leq k$. Similarly, the MS is assigned to BS_j if and only if $\mathbf{X}[k \backslash k+1] \in \mathbf{J}_0\mathbf{H}^k$ or $\mathbf{X}[k \backslash r] \in \mathbf{J}\mathbf{H}^{r-1}$ for some r, where $1 \leq r \leq k$.

Proof: Suppose $\mathbf{X}[k \backslash r] \in \mathbf{I}\mathbf{H}^{r-1}$, where $1 \leq r \leq k$. This condition is equivalent to $\mathbf{X}[k-r+1] \in \mathbf{I}$ and $\mathbf{X}[l] \in \mathbf{H}$, $l = k-r+2, \ldots, k$. Clearly, the MS is assigned to BS_i at time $k-r+1$. Since no handoff occurs at times $l = k-r+2, \ldots, k$, the MS must also be assigned to BS_i at times $l = k-r+2, \ldots, k$. Similarly, if $\mathbf{X}[k \backslash k+1] \in \mathbf{I}_0\mathbf{H}^k$, then the MS must be assigned to BS_i at time k.

Conversely, assume that the MS is assigned to BS_i at time k. Then, we must have $\mathbf{X}[l] \in \mathbf{I}$ for some $1 \leq l \leq k$ or $\mathbf{X}[l] \in \mathbf{I}_0$ for $l=0$. Let l^* be the largest such l. Since the MS is assigned to BS_i at time k, it must be that $\mathbf{X}[m] \in \mathbf{H}$, $m = l^*+1, \ldots, k$. Setting $r = k - l^* + 1$, we have that $\mathbf{X}[k \backslash r] \in \mathbf{I}_0\mathbf{H}^{r-1}$ when $r = k+1$, or $\mathbf{X}[k \backslash r] \in \mathbf{I}\mathbf{H}^{r-1}$ otherwise. The case of assignment of MS to BS_j at time k is proved similarly. ■

Let $E_i[k]$ denote the event that the mobile is assigned to BS_i at time k. We refer to $E_i[k]$ as the cell i assignment event at time k. By virtue of Proposition 1, we can express the assignment event $E_i[k]$ as a disjoint union of more elementary events[2]

$$E_i[k] = \{\mathbf{X}[k \backslash k+1] \in \mathbf{I}_0\mathbf{H}^k\} \sqcup \bigsqcup_{r=1}^{k} \{\mathbf{X}[k \backslash r] \in \mathbf{I}\mathbf{H}^{r-1}\}. \tag{12}$$

For convenience, we introduce the notation

$$p_k(\mathbf{S}) = \Pr\{\mathbf{X}[k \backslash |\mathbf{S}|] \in \mathbf{S}\}$$

where $\mathbf{S}$ is a string of symbols on the assignment alphabet $\mathcal{A}$ with length denoted by $|\mathbf{S}|$. Noting that the events on the right-hand side of (12) are mutually exclusive, we obtain the following exact characterization of the cell assignment probabilities.

Proposition 2: The cell assignment probabilities can be expressed as

$$P_i[k] = p_k(\mathbf{I}_0\mathbf{H}^k) + \sum_{r=1}^{k} p_k(\mathbf{I}\mathbf{H}^{r-1}) \tag{13}$$

$$P_j[k] = p_k(\mathbf{J}_0\mathbf{H}^k) + \sum_{r=1}^{k} p_k(\mathbf{J}\mathbf{H}^{r-1}). \tag{14}$$

[2]When sets A and B are disjoint we denote their union by $A \bigsqcup B$ to emphasize this property.

D. Handoff Probability

Let $E_{ij}[k]$ denote the event that at time k the cell assignment changes from cell i to cell j, i.e., a handoff occurs from cell i to cell j. Similarly, $E_{ji}[k]$ denotes the event that a handoff occurs from cell j to cell i at time k. We can express the cell handoff events, $E_{ij}[k]$ and $E_{ji}[k]$ for $k \geq 1$, in terms of the cell assignment events defined earlier as

$$E_{ij}[k] = E_i[k-1] \cap E_j[k]$$

and

$$E_{ji}[k] = E_j[k-1] \cap E_i[k].$$

Analogous to Proposition 2, the conditions for a handoff event to occur can be expressed as follows.

Proposition 3: For $k \geq 1$, a handoff from i to j occurs at time k if and only if $\mathbf{X}[k] \in \mathbf{J}$ and $\mathbf{X}[k-1 \backslash r-1] \in \mathbf{I}\mathbf{H}^{r-2}$ for some r, $2 \leq r \leq k+1$ or $\mathbf{X}[k-1 \backslash k] \in \mathbf{I}_0\mathbf{H}^{k-1}$. Similarly, a handoff from BS_j to BS_i occurs at time k if and only if $\mathbf{X}[k] \in \mathbf{I}$ and $\mathbf{X}[k-1 \backslash r-1] \in \mathbf{J}\mathbf{H}^{r-2}$ for some r, $2 \leq r \leq k+1$, or $\mathbf{X}[k-1 \backslash k] \in \mathbf{J}_0\mathbf{H}^{k-1}$.

Hence, the handoff events $E_{ij}[k]$ and $E_{ji}[k]$, for $k \geq 1$, can be expressed as

$$E_{ij}[k] = \{\mathbf{X}[k \backslash k+1] \in \mathbf{I}_0\mathbf{H}^{k-1}\mathbf{J}\} \sqcup \bigsqcup_{r=2}^{k} \{\mathbf{X}[k \backslash r] \in \mathbf{I}\mathbf{H}^{r-2}\mathbf{J}\} \tag{15}$$

$$E_{ji}[k] = \{\mathbf{X}[k \backslash k+1] \in \mathbf{J}_0\mathbf{H}^{k-1}\mathbf{I}\} \sqcup \bigsqcup_{r=2}^{k} \{\mathbf{X}[k \backslash r] \in \mathbf{J}\mathbf{H}^{r-2}\mathbf{I}\}. \tag{16}$$

Since the events on the right-hand sides of (15) and (16) are mutually exclusive, we have the following exact characterization of the cell handoff probabilities, analogous to Proposition 2.

Proposition 4: The cell handoff probabilities for $k \geq 1$ can be expressed as

$$P_{ij}[k] = p_k(\mathbf{I}_0\mathbf{H}^{k-1}\mathbf{J}) + \sum_{r=2}^{k} p_k(\mathbf{I}\mathbf{H}^{r-2}\mathbf{J})$$

$$P_{ji}[k] = p_k(\mathbf{J}_0\mathbf{H}^{k-1}\mathbf{I}) + \sum_{r=2}^{k} p_k(\mathbf{J}\mathbf{H}^{r-2}\mathbf{I}). \tag{17}$$

E. Other Performance Metrics

An important performance measure is the mean number of handoffs that occur as the mobile moves along a given trajectory. Let N_{ho} denote the number of handoffs that occur for a mobile moving along a given trajectory. Let 1_E denote the indicator random variable for the event E. The number of handoffs can be expressed as

$$N_{\mathrm{ho}} = \sum_{k=1}^{K} \left(1_{E_{ij}[k]} + 1_{E_{ji}[k]}\right).$$

Hence, the mean number of handoffs is given by

$$E[N_{\text{ho}}] = \sum_{k=1}^{K}(P_{ij}[k] + P_{ji}[k]) = \sum_{k=1}^{K} P_{\text{ho}}[k]$$

where $P_{\text{ho}}[k]$ is the probability of handoff in either direction at time k. Finally, the *crossover point* is defined as the point along a straight-line trajectory at which the probability of the MS being assigned to BS_i drops below 0.5 (cf., [6]), given that the probability of assignment to BS_i at time $k = 0$ is greater than 0.5. The crossover point is a measure of the handoff delay.

IV. Numerical Evaluation of Handoff Performance

For handoff algorithms based on relative signal strength, the handoff behavior of the MS maps to the 1-D process $X_\Delta[k] = X_i[k] - X_j[k]$. In this case, the assignment regions are intervals of the real line: $I = [h_i, \infty)$, $J = (-\infty, h_j]$, and $H = (-h_j, h_i)$. The assignment regions at system initialization time are $I_0 = (0, \infty)$ and $J_0 = (-\infty, 0)$. The expressions derived earlier for assignment and handoff probability map straightforwardly to the 1-D case. In this case, (13) expresses the cell assignment probability to BS_i at time k as a summation of probabilities of the form $p_k(IH^{r-1})$. The process $\{X_\Delta[k]\}$ satisfies a difference equation similar to (10) as follows for $k \geq 2$:

$$X_\Delta[k] = (a+b)X_\Delta[k-1] - abX_\Delta[k-2] + \frac{d_s}{d_{\text{av}}}(m_\Delta[k] - am_\Delta[k-1]) + \frac{d_s}{d_{\text{av}}}V_\Delta[k] \quad (18)$$

where $m_\Delta[k] = m_i[k] - m_j[k]$ and $V_\Delta[k] = V_i[k] - V_j[k]$. Thus, $\{X_\Delta[k]\}$ can be characterized as a second-order AR process.

By exploiting the second-order Markov property of $\{X_\Delta[k]\}$, we can develop a recursive procedure for evaluating the assignment and handoff probabilities. We define a sequence of bivariate functions $\{g_k(x_{k-1}, x_k), k \geq 1\}$ as follows:

$$g_1(x_0, x_1) = f_1(x_0, x_1)$$
$$g_2(x_1, x_2) = \int_{I_0} g_1(x_0, x_1) f_2(x_2|x_0, x_1)dx_0 \quad (19)$$

and for $k \geq 3$

$$g_k(x_{k-1}, x_k) = \int_I f_{k-1}(x_{k-2}, x_{k-1}) \times f_k(x_k|x_{k-2}, x_{k-1})dx_{k-2} + \int_H g_{k-1}(x_{k-2}, x_{k-1}) \times f_k(x_k|x_{k-2}, x_{k-1})dx_{k-2}. \quad (20)$$

Here, $f_k(x_{k-1}, x_k)$ denotes the joint density of $\{X_\Delta[k-1], X_\Delta[k]\}$ and $f_k(x_k|x_{k-2}x_{k-1})$ denotes the conditional density of $X_\Delta[k]$ given $X_\Delta[k-1]$ and $X_\Delta[k-2]$. Expressions for the conditional joint densities are derived in Appendix II. The notation $\int_A$ denotes the standard Riemann integral over the set A. The bivariate functions g_k have the following useful property (the proof can be found in Appendix III).

Lemma 1: For $k \geq 2$

$$\int_H \int_H g_k(x_{k-1}, x_k)dx_k dx_{k-1} = p_k(I_0H^k) + \sum_{r=3}^{k} p_k(IH^{r-1}) \triangleq G_k. \quad (21)$$

The probabilities of the form $p_k(S)$, where S is a string of characters representing intervals of the real line, are expressed by (36) in Appendix III.

Applying Proposition 2 and Lemma 1, we can express the probability of assignment to BS_i as follows (the result for assignment to BS_j is analogous).

Proposition 5:

$$P_i[k] = P_k(I) + P_k(IH) + \int_H \int_H g_k(x_{k-1}, x_k)dx_k dx_{k-1}, \quad k \geq 2 \quad (22)$$

with the initial conditions $P_i[1] = p_1(I) + p_1(I_0H)$ and $P_i[0] = p_0(I_0)$.

The handoff probability from BS_i and BS_j can also be expressed in terms of the functions g_k (the result for handoff from BS_j to BS_i is analogous).

Proposition 6:

$$P_{ij} = P_1(i_0J) \quad (23)$$
$$P_{ij}[k] = P_k(IJ) + \int_H \int_J g_k(x_{k-1}, x_k)dx_k dx_{k-1} \quad (24)$$

for $k \geq 2$.

In a practical implementation of the recursive procedure for evaluating assignment and handoff probabilities, the bivariate function $g_k(x_{k-1}, x_k)$ can be represented as a matrix over a finite grid of points in 2-D space. The integrals that appear in the recursive procedure are approximated by trapezoidal integration. The numerical procedure can be made arbitrarily more accurate by using a larger matrix, corresponding to a grid of higher granularity. Our implementation of the procedure computes assignment probabilities to an error of less than 10^{-6}. The overall computational complexity of the procedure at each iteration is $O(h^2)$, where h denotes the hysteresis parameter.

V. Numerical Results

We now present numerical results to validate the accuracy of our numerical procedure for evaluating handoff performance. We evaluate the cell assignment and handoff probabilities along a straight-line trajectory between two BSs BS_i and BS_j. We also evaluate the impact of the hysteresis parameter h on the mean number of handoffs and the crossover point for the two trajectories. We set the main system parameters as follows: $D = 2000$ m, $\kappa_1 = 0$ dB, $\kappa_2 = 30$ dB, $\sigma_{W_i} = 6$ dB, $d_o = 20$ m, $d_s = 1$ m. The averaging parameter d_{av} is set to 10 m.

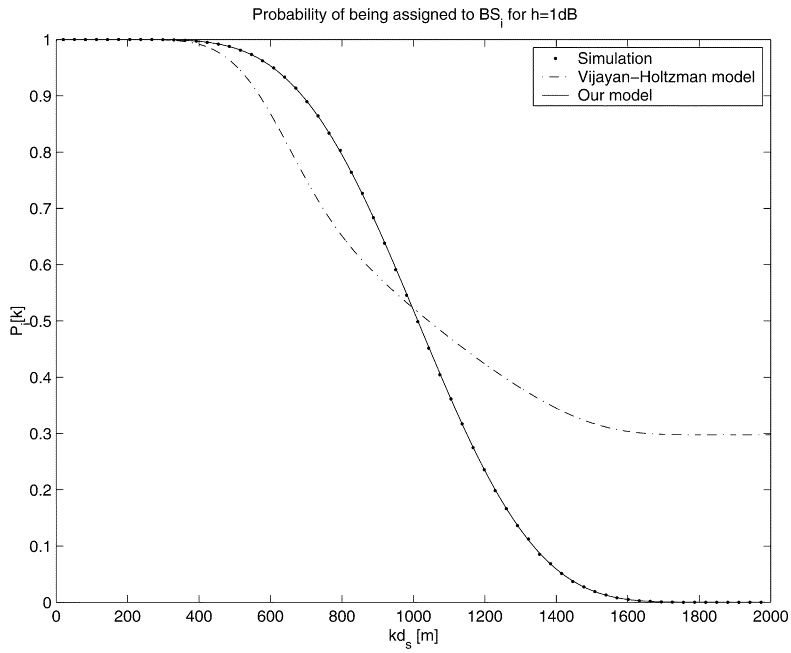

Fig. 6. Probability of being assigned to station BS_i with $h = 1$ dB.

We validated our numerical procedure against results obtained using computer simulation. Each simulation data point was obtained by performing 100 000 sample path realizations. The 95% confidence intervals were computed but are too small to be displayed except for in Fig. 8, where handoff probabilities are plotted. The simulation results validate the accuracy of our numerical procedure (and vice versa). The numerical procedure is far more efficient than simulation, since the performance metrics are only computed along a single realization of the MS trajectory, whereas a large number of sample path realizations are required to achieve an equivalent level of accuracy using the simulation approach. For comparison purposes, we also obtained numerical results using the Poisson approximation model of Vijayan and Holtzman [6] and the approximate discrete-time model of Zhang and Holtzman [7] (without absolute thresholds).

Fig. 6 shows the probability that the MS is assigned to BS_i as a function of the sampled distance along the straight-line trajectory from BS_i to BS_j when the hysteresis parameter is set to $h = 1$ dB. The curve obtained from our model matches closely to that obtained from simulation. Since the MS begins at BS_i, the assignment probability is initially one and then decreases monotonically to zero as it approaches BS_j along the straight-line trajectory. The cell assignment probability curve obtained using the Vijayan–Holtzman model is also shown in Fig. 6. The assignment probabilities obtained from Vijayan–Holtzman model are inaccurate in this scenario and a bias can be seen in the crossover point. For relatively small hysteresis levels, the Vijayan–Holtzman model does not provide a good estimate for the crossover point and the mean number of handoffs.

Observe in Fig. 6 that the crossover point is approximately equal to the halfway point along the trajectory, i.e., 1000 m. The ideal assignment probability curve along the direct trajectory is a step function with a step discontinuity from level 1 to level 0 at the halfway point. As the hysteresis level h is increased, the assignment probability curve more closely approximates a step function. However, the value of the crossover point also increases, implying a larger handoff delay in this case. Therein lies a critical tradeoff in dimensioning the parameter h for hysteresis-based handoff algorithms.

For larger values of h one would expect the Vijayan–Holtzman results to improve since the Poisson level-crossing model is asymptotically accurate as the value of the parameter h is increased. However, Fig. 7 shows significant discrepancies for $h = 12$ dB when the MS moves along the 45° line trajectory indicated in Fig. 1. In Fig. 7, there is a significant error in the assignment probability curve for the first couple of hundred meters, which is approximately the radius of a microcell. This is because the asymptotic model used in [6] does not take into account the transient behavior due to system initialization when the MS becomes active. This effect is more pronounced for larger values of h.

Fig. 8 shows the probability of the MS being handed off from BS_i to BS_j as it moves along the trajectory when the hysteresis parameter is set to $h = 3$ dB. The simulation results are shown along with 95% confidence intervals. The curve obtained from the Vijayan–Holtzman model underestimates the handoff probabilities. The handoff probability increases to a maximum value near the crossover point. It should further be noted that for small values of the handoff probabilities, an especially large number of simulations is required to achieve an equivalent level of accuracy, making our analytical approach an attractive alternative to simulation.

In Fig. 9, the mean number of handoffs for an MS is plotted as a function of the hysteresis parameter h using the four methods discussed above. Note that the Zhang–Holtzman model [7] overestimates the mean number of handoffs over almost the entire range of hysteresis values. The Vijayan–Holtzman model underestimates the mean number of handoffs when h is less than

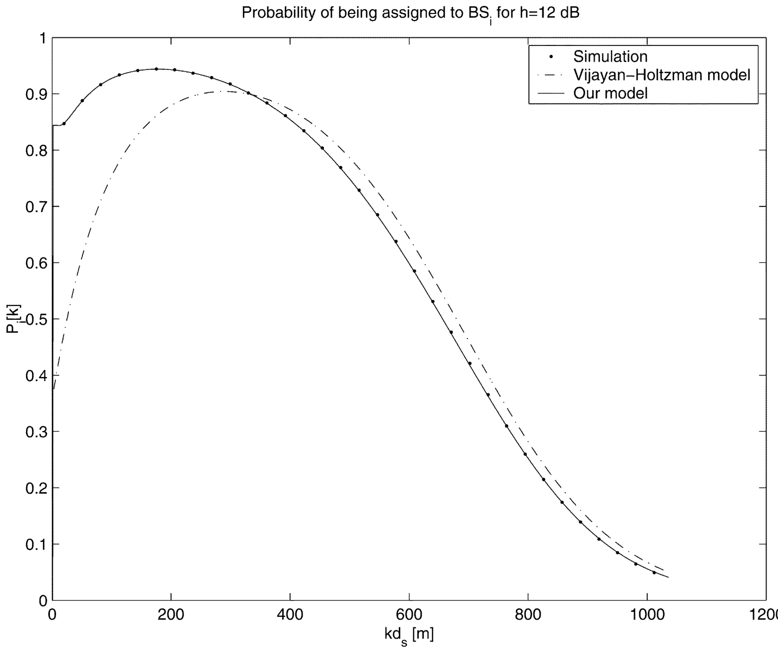

Fig. 7. Probability of being assigned to station BS_i with $h = 12$ dB for 45° trajectory.

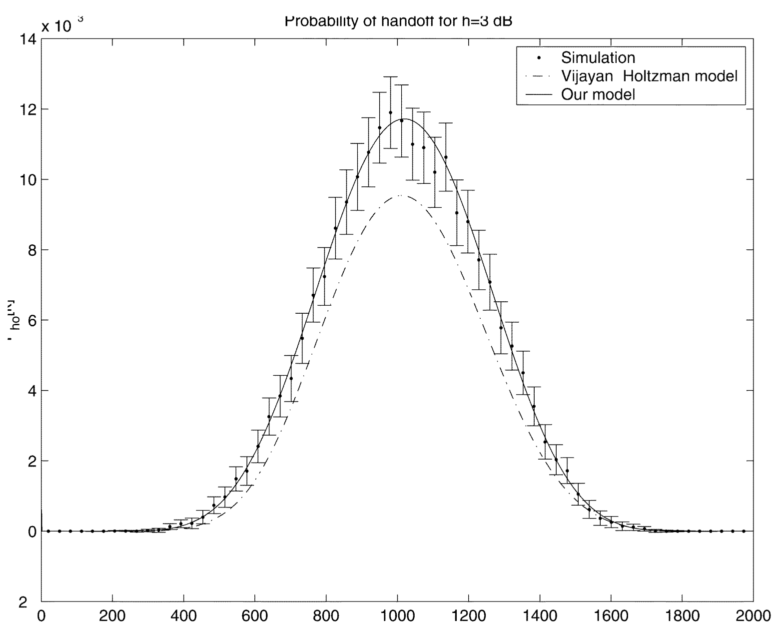

Fig. 8. Probability of handoff from BS_i to BS_j with $h = 3$ dB.

5 dB, while for $h > 5$ dB, this model shows close agreement with our analytical results.

In general, it is desirable to minimize the number of handoffs while maintaining as small a handoff delay as possible. A small handoff delay is particularly important for the design and dimensioning of 3G systems, since the allocated bandwidth is significantly larger than for 2G systems. As we saw earlier, small handoff delay can be achieved by using small values for the hysteresis parameter. On the other hand, small hysteresis levels imply a larger number of handoffs. The tradeoff between crossover point and mean number of handoffs is illustrated explicitly in Fig. 10. The optimum operating point will typically lie in the neighborhood of the knee of the tradeoff curve. For reference, the hysteresis level corresponding to a given crossover point is also plotted on the same graph.

VI. Conclusion

The main contribution of this paper is a rigorous discrete-time approach to analyze the handoff performance of an MS moving along a trajectory in a cellular network. In this approach, the processed relative signal strength observed by an MS along a trajectory is mapped to a random sequence over a set of assignment regions. Based on the proposed discrete-time framework, expressions were derived for the probabilities of cell assignment and

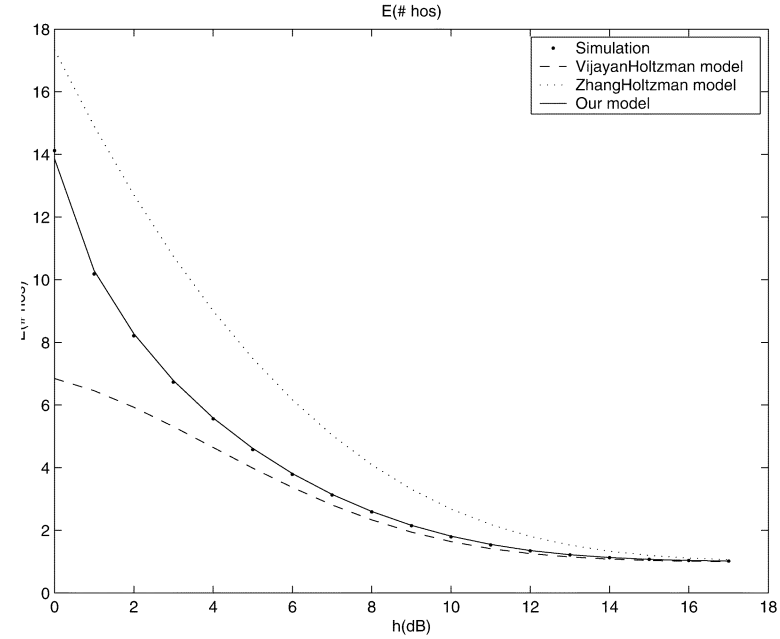

Fig. 9. Mean number of handoffs versus hysteresis level.

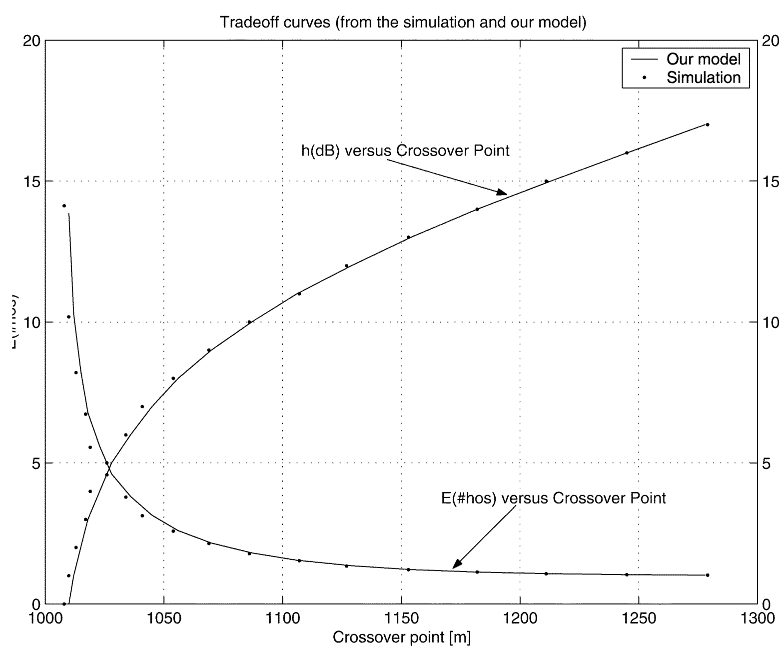

Fig. 10. Crossover point versus mean number of handoffs.

handoff along arbitrary straight-line trajectories. An efficient numerical procedure was developed for accurately evaluating the performance measures for handoff algorithms based on relative signal strength. Our results find direct application to the design and dimensioning of hard handoff algorithms in cellular networks based on the GSM, GPRS, and UMTS (FMA1 mode) standards (cf., [1]).

In recent years, some novel handoff algorithms have been proposed in the research literature. Veeravalli and Kelly [19], for example, formulate a locally optimal hard handoff algorithm to obtain the best tradeoff between expected number of service failures and expected number of handoffs. Akar and Mitra [21] consider further variations in optimal and suboptimal hard handoff control algorithms. Pahlavan *et al.* [10] and Narishiman and Cox [22] suggest the use of neural networks to make handoff decisions. Such handoff algorithms generally result in nonlinear assignment regions (cf., Fig. 4). In principle, nonlinear assignment regions are accommodated in our discrete-time framework, but the numerical evaluation of the assignment and handoff probabilities in this case may be computationally challenging. The same remark applies to handoff algorithms that use both relative and absolute signal strengths (cf., Fig. 3).

Our discrete-time framework can also accommodate changes in the velocity of the MS. In this case, the statistics of the pilot signal strength measurements would be nonstationary, but our recursive numerical procedure could still be applied by appropriately specifying the second-order density functions. An interesting avenue of investigation is to extend our approach to analyze adaptive handoff algorithms (cf., [23]–[25]).

In the present paper, we exploited the second-order Markov property of the processed relative signal strength $\{X_\Delta[k]\}$ to carry out the handoff analysis. In [26], this key observation is used to develop an alternative averaging technique to eliminate fast fading while preserving the first-order Markov property of the raw signal strength. In this case, the handoff analysis can be carried out even more efficiently than with conventional averaging. Finally, we remark that although the present paper has focused on the problem of hard handoff, the discrete-time handoff approach can be applied to the analysis of soft handoff algorithms as well [27].

Appendix I
Difference Equation for $\{X_i[k]\}$

From (7), we see that the shadow fading process $\{W_i[k]\}$ is obtained by passing the Gaussian noise process $\{V_i[k]\}$ through a first-order filter. In the Z-transform domain, we have

$$W_i(z) = F_0(z)V_i(z) \tag{25}$$

where $W_i(z)$ denotes the (unilateral) Z-transform of $\{W_i[k]\}$, $V_i(z)$ denotes the Z-transform of $\{V_i[k]\}$, and $F_0(z)$ is the Z-transform of the first-order filter, given by $F_0(z) = [1 - az^{-1}]^{-1}$. In the Z-domain, the raw pilot signal strength can be expressed as

$$Y_i(z) = M_i(z) + F_0(z)V_i(z) \tag{26}$$

where $M_i(z)$ is the Z-transform of the mean signal strength $\{m_i[k]\}$. Taking the Z-transform of both sides, we have

$$X_i(z) = F_{\rm av}(z)Y_i(z) \tag{27}$$

with $F_{\rm av}(z) = d_s[1 - bz^{-1}]^{-1}/d_{\rm av}$. Solving for $Y_i(z)$ in (27), we obtain $Y_i(z) = d_{\rm av}(1 - bz^{-1})X_i(z)/d_s$. Combining (26) and (27), we have

$$X_i(z) = F_{\rm av}(z)M_i(z) + F_{\rm av}(z)F_o(z)V_i(z). \tag{28}$$

Dividing both sides of (28) by $d_{\rm av}F_{\rm av}(z)F_0(z)/d_s$, we obtain

$$(1 - az^{-1})(1 - bz^{-1})X_i(z) = \frac{d_s}{d_{\rm av}}[(1 - az^{-1})M_i(z) + V_i(z)]. \tag{29}$$

Now reverting back to the discrete-time domain, we obtain the second-order recurrence (10).

Appendix II
Statistics of the Processed Signal Strength

Let $\bar{m}[k]$ denote the mean of $X_i[k]$. From (28), the Z-transform of the process $\{\bar{m}[k]\}$ can be expressed as $\bar{M}_i(z) = F_{\rm av}(z)M_i(z)$. Reverting to the time domain, we can express $\bar{m}[k]$ as

$$\bar{m}[k] = \frac{\bar{m}[k-1] + d_s m[k]}{d_{\rm av}}, \quad k \geq 0. \tag{30}$$

The autocovariance function $K_{X_i}(m)$ of $\{X_i[k]\}$ is equivalent to the autocorrelation of the zero-mean process $\{\tilde{X}_i[k]\}$, where $\tilde{X}_i[k] = X_i[k] - \bar{m}_i[k]$. The process $\{\tilde{X}_i[k]\}$ satisfies the recurrence relation [cf., (10)]

$$\tilde{X}_i[k] = \frac{(a+b)\tilde{X}_i[k-1] - ab\tilde{X}_i[k-2] + d_sV_i[k]}{d_{\rm av}}, \quad k \geq 2. \tag{31}$$

The autocovariance function of $\{X_i[k]\}$ is then given by

$$K_{X_i}(l) = E\{\tilde{X}_i[k-l]\tilde{X}_i[k]\}. \tag{32}$$

When $l \geq 1$, $V_i[k]$ and $\tilde{X}_i[k-l]$ are independent and we have

$$K_{X_i}(l) = (a+b)K_{X_i}(l-1) - abK_{X_i}(l-2). \tag{33}$$

Note that $K_{X_i}(0) = \sigma^2_{X_i}$. Setting $l = 1$ in (33) we obtain

$$K_{X_i}(1) = \frac{a+b}{1+ab}\sigma^2_{X_i}. \tag{34}$$

The correlation coefficient is given by

$$\rho_{X_i} = \frac{K_{X_i}(1)}{\sigma^2_{X_i}} = \frac{a+b}{1+ab}.$$

Taking the variance on both sides of (31) we obtain

$$\sigma^2_{X_i} = \frac{\frac{d_s^2\sigma^2_{V_i}}{d^2_{\rm av}}}{\frac{1-a^2b^2-(a+b)^2(1-ab)}{(1+ab)}}. \tag{35}$$

Equations (33)–(35) completely define the autocovariance function $K_{X_i}(l)$.

Since $\{X_i[k]\}$ and $\{X_j[k]\}$ are assumed to be independent, it follows that the autocovariance function of the processed relative signal strength $\{X_\Delta[k]\}$ is given by $K_{X_\Delta}(l) = K_{X_i}(l) + K_{X_j}(l)$. If we further assume that $\sigma_{V_i} = \sigma_{V_j}$, then the variance of $V_\Delta[k]$ is given by $\sigma^2_{V_\Delta} = 2\sigma^2_{V_i}$ and $K_{X_\Delta}(l) = 2K_{X_i}(l) = 2K_{X_j}(l)$. In particular, we have $\sigma^2_{X_\Delta} = 2\sigma^2_{X_i}$. Also, in this case the correlation coefficient is given by $\rho_{X_\Delta} = \rho_{X_i} = \rho_{X_j}$.

The joint density $f_k(x_{k-1}, x_k)$ is a bivariate Gaussian density with correlation coefficient given by ρ_{X_Δ}. The conditional density $f_k(x_k|x_{k-2}, x_{k-1})$ is a Gaussian density with mean given by

$$\mu_k(x_k|x_{k-2}, x_{k-1}) = \frac{(a+b)x_{k-1} - abx_{k-2} + d_s(m_\Delta[k] - am_\Delta[k-1])}{d_{\rm av}}$$

and standard deviation given by

$$\sigma_k(x_k|x_{k-2},x_{k-1}) = \frac{d_s \sigma_{V_\Delta}}{d_{\text{av}}}.$$

Appendix III
Proof of Lemma 1

We introduce the following compact notation for a multidimensional integral over the intervals $A_1,\ldots,A_n$ of the real line

$$\int_{A_1\cdots A_n} g(x_1,\ldots,x_n)dx_{[n\backslash n]} \triangleq \int_{A_1}\cdots\int_{A_n} g(x_1,\ldots,x_n)dx_1\ldots dx_n.$$

Let $S = A_1\cdots A_n$ be a string of symbols, each of which represents an interval of the real line. Then, the probability $p_k(S)$ can be expressed as

$$p_k(S) = \int_S f_k(x_{k-n+1},\ldots,x_k)dx_{[k\backslash n]} \quad (36)$$

for $k \geq n-1$.

For $k=2$, the left-hand side of (21) is given by

$$\begin{aligned} G_2 &= \int_{H^2} g_2(x_1,x_2)dx_{[2\backslash 2]} \\ &= \int_{H^2 I_0} f_1(x_0,x_1)f_2(x_2|x_0,x_1)dx_{[2\backslash 3]} = p_k(I_0H^2). \end{aligned}$$

For $k \geq 3$, we have

$$\begin{aligned} G_k &= \int_{H^2} g_k(x_{k-1},x_k)dx_{[k\backslash 2]} \\ &= \int_{H^2 I} f_{k-1}(x_{k-2},x_{k-1})f_k(x_k|x_{k-2},x_{k-1})dx_{[k\backslash 3]} \\ &\quad + \int_{H^3} g_{k-1}(x_{k-2},x_{k-1})f_k(x_k|x_{k-2},x_{k-1})dx_{[k\backslash 3]} \\ &= p_k(IH^2) + \int_{H^3 I} f_{k-2}(x_{k-3},x_{k-2}) \\ &\quad \times f_{k-1}(x_{k-1}|x_{k-3},x_{k-2})f_k(x_k|x_{k-2},x_{k-1})dx_{[k\backslash 4]} \\ &\quad + \int_{H^4} g_{k-2}(x_{k-3},x_{k-2})f_{k-1}(x_{k-1}|x_{k-3},x_{k-2}) \\ &\quad \times f_k(x_k|x_{k-2},x_{k-1})dx_{[k\backslash 4]}. \end{aligned} \quad (37)$$

Using the fact that the process $\{X_\Delta[k]\}$ is a second-order Markov chain, the integrand of the second term in (37) reduces to the joint pdf $f_k(x_{[k\backslash 4]})$. Hence, the second term is simply $p_k(IH^3)$. By expanding the third term in (37) and using the second-order Markov property of $\{X_\Delta[k]\}$ in a recursive fashion, we obtain

$$\begin{aligned} G_k &= p_k(IH^2) + \cdots + p_k(IH^{k-1}) \\ &\quad + \int_{H^k}\int_{I_0} g_1(x_0,x_1)f_k(x_2,\ldots,x_k|x_0,x_1)dx_{[k\backslash k+1]} \\ &= \sum_{r=3}^{k} p_k(IH^{r-1}) + p_k(I_0H^k). \end{aligned}$$

References

[1] V. K. Garg, *Wireless Network Evolution 2G to 3G*. Upper Saddle River, NJ: Prentice-Hall, 2002.

[2] R. Beck and H. Panzer, “Strategies for handover and dynamic channel allocation in micro-cellular mobile radio systems,” in *Proc. IEEE Vehicular Technol. Conf. (VTC’89)*, May 1989, pp. 178–185.

[3] B. Gudmundson and O. Grimlund, “Handoff in microcellular based personal telephone systems,” in *Proc. WINLAB Workshop* , East Brunswick, NJ, Oct. 1990.

[4] W. R. Mende, “On the hand-over rate in future cellular systems,” in *Proc. 8th Eur. Conf. Area Commun. (EUROCON)*, June 1988, pp. 358–361.

[5] ——, “Evaluation of a proposed handover algorithm for the gsm cellular system,” in *Proc. IEEE Vehicular Technol. Conf. (VTC)*, May 1990, pp. 264–269.

[6] R. Vijayan and J. M. Holtzman, “A model for analyzing handoff algorithms,” *IEEE Trans. Veh. Technol.*, vol. 42, pp. 351–356, Aug. 1993.

[7] N. Zhang and J. M. Holtzman, “Analysis of handoff algorithms using both absolute and relative measurements,” *IEEE Trans. Veh. Technol.*, vol. 45, pp. 174–179, Feb. 1996.

[8] G. P. Pollini, “Trends in handover design,” *IEEE Commun. Mag.*, vol. 34, pp. 82–90, Mar. 1996.

[9] N. D. Tripathi, J. H. Reed, and H. F. VanLandingham, “Handoff in cellular systems,” *IEEE Personal Commun.*, vol. 5, pp. 26–37, Dec. 1998.

[10] K. Pahlavan *et al.*, “Handoff in hybrid mobile data networks,” *IEEE Personal Commun.*, vol. 7, pp. 34–37, Apr. 2000.

[11] G. P. Pollini, “Handover rates in cellular systems: Toward a closed form approximation,” in *Proc. IEEE Globecom*, vol. 2, 1997, pp. 711–715.

[12] S. Ulukus and G. P. Pollini, “Handover delay in cellular wireless systems,” in *Proc. IEEE Int. Conf. Communications (ICC)*, vol. 3, 1998, pp. 1370–1374.

[13] S. Mukherjee and D. Avidor, “Dynamics of path losses between a mobile terminal and multiple base stations in a cellular environment,” *IEEE Trans. Veh. Technol.*, vol. 50, pp. 1590–1603, Nov. 2001.

[14] D. Tcha, S. Kang, and G. Jin, “Load analysis of the soft handoff in a CDMA cellular system,” *IEEE J. Select. Areas Commun.*, vol. 19, pp. 1147–1152, June 2001.

[15] R. P. Narrainen and F. Takawira, “Performance analysis of soft handoff in CDMA cellular networks,” *IEEE Trans. Veh. Technol.*, vol. 50, pp. 1507–1517, Nov. 2001.

[16] D. Hong and S. S. Rappaport, “Traffic model and performance analysis for cellular mobile radio telephone systems with prioritized and nonprioritized handoff procedures,” *IEEE Trans. Veh. Technol.*, vol. 35, pp. 77–92, Aug. 1986.

[17] R. A. Guerin, “Channel occupancy time distribution in a cellular radio system,” *IEEE Trans. Veh. Technol.*, vol. 35, pp. 89–99, Aug. 1987.

[18] M. Gudmundson, “Correlation model for shadowing fading in mobile radio systems,” *Electron. Lett.*, vol. 27, pp. 2145–2146, Nov. 1991.

[19] V. V. Veeravalli and O. E. Kelly, “A locally optimal handoff algorithm for cellular communications,” *IEEE Trans. Veh. Technol.*, vol. 46, Aug. 1997.

[20] I. F. Blake and W. C. Lindsey, “Level-crossing problems for random processes,” *IEEE Trans. Inform. Theory*, vol. 19, pp. 295–315, May 1973.

[21] M. Akar and U. Mitra, “Variations on optimal and suboptimal handoff control for wireless communication systems,” *IEEE J. Select. Areas Commun.*, vol. 19, pp. 1173–1185, June 2001.

[22] R. Narashiman and D. Cox, “A handoff algorithm for wireless systems using pattern recognition,” in *Proc. IEEE Int. Symp. Pers., Indoor, and Mobile Radio Commun. (PIMRC)*, vol. 1, 1998, pp. 335–339.

[23] J. M. Holtzman and A. Sampath, “Adaptive averaging methodology for handoffs in cellular systems,” *IEEE Trans. Veh. Technol.*, vol. 44, Feb. 1995.

[24] M. D. Austin and G. L. Stüber, “Velocity adaptive handoff algorithms for microcellular systems,” in *Proc. Int. Conf. Univ. Pers. Comm.*, Ottawa, Canada, Oct. 1993, pp. 793–797.

[25] R. Prakash and V. V. Veeravalli, “Adaptive hard handoff algorithms,” *IEEE J. Select. Areas Commun.*, vol. 18, pp. 2456–2464, Nov. 2000.

[26] A. E. Leu and B. L. Mark, “Modeling and analysis of fast handoff algorithms for microcellular networks,” in *Proc. IEEE Int. Symp. Modeling, Analysis, Simulation Comp. Telecomm. Syst. (MASCOTS)*, Oct. 2002, pp. 321–328.

[27] ——, “Discrete-time analysis of soft handoff in CDMA cellular networks,” in *Proc. IEEE Int. Conf. Communications (ICC)*, New York, Apr./May 2002, pp. 3222–3226.

Alexe E. Leu (S'97–M'04) received the Diploma Engineer in applied telecommunications and the M.Sc. degree in signal processing from Polytechnic University of Bucharest, Bucharest, Romania, in 1995 and 1996, respectively. He received the Ph.D. degree from George Mason University, Fairfax, VA, in 2003.

From 1999 to 2001, he was a Design Engineer in the R&D Department, LCC International, Inc., McLean. Since March 2004, he has been with the Shared Spectrum Company, Vienna, VA, working as a Principal Engineer on the DARPA XG program. His research interests include cognitive radios and frequency agile spectrum sharing.

Brian L. Mark (M'91) received the B.A.Sc. degree in computer engineering with an option in mathematics from the University of Waterloo, Ontario, Canada, in 1991 and the Ph.D. degree in electrical engineering from Princeton University, Princeton, NJ, in 1995.

He was a Research Staff Member at the C&C Research Laboratories, NEC, USA, from 1995 to 1999. In 1999, he was on part-time leave from NEC as a Visiting Researcher at Ecole Nationale Supérieure des Télécommunications, Paris, France. In 2000, he joined the Department of Electrical and Computer Engineering, George Mason University, where he is currently an Assistant Professor. His research interests include the design, modeling, and analysis of computer systems and communication network architectures.

Dr. Mark was corecipient of the best conference paper award for IEEE Infocom'97. He received a National Science Foundation CAREER Award in 2002.